PCCP

An upper limit to the concentration of an SO_2 complex at the air–water interface at 298 K: infrared experiments and *ab initio* calculations

Husheng Yang,†[a] Nicholas J. Wright,[ab] Aaron M. Gagnon,‡[c] R. Benny Gerber*§[ab] and Barbara J. Finlayson-Pitts*§[a]

[a] *Department of Chemistry, University of California, Irvine, CA 92697-2025, USA*
[b] *Department of Physical Chemistry and The Fritz Haber Research Center, The Hebrew University, Jerusalem, Israel 91904*
[c] *Thermo Spectra-Tech, 230 Long Hill Cross Road, Shelton, CT 06484, USA*

Received 2nd October 2001, Accepted 12th February 2002
First published as an Advance Article on the web 16th April 2002

Unique reactions occurring at the interface between air and aqueous solutions are increasingly recognized to be of potential importance in atmospheric processes. Sulfur dioxide was one of the first species for which experimental evidence for the existence of a surface complex was obtained by several different groups, based on the kinetics of SO_2 uptake into aqueous solutions, large decreases in surface tension and second harmonic generation spectroscopic studies. The uptake has been proposed to involve an uncharged surface complex which subsequently converts into ionic species. We report here the results of a search for an uncharged SO_2 complex at or near the surface using attenuated total reflectance Fourier transform infrared spectrometry (ATR-FTIR) at 298 K guided by *ab initio* calculations of a 1:1 SO_2–H_2O complex. No infrared absorption bands attributable to such a complex of SO_2 were observed experimentally in the expected region, giving an upper bound of 4×10^{14} SO_2 cm^{-2} to the concentration of neutral SO_2 molecules weakly sorbed to the surface in equilibrium with ~1 atm SO_2(g). The implications for the nature of the surface species and previous observations are discussed.

Introduction

The uptake of gases into liquids, followed by diffusion and reactions in the liquid phase, is known to be important in a number of atmospheric processes. For example, the uptake of gaseous SO_2 into fogs and clouds followed by its oxidation by H_2O_2 and O_3 in the liquid phase is a major source of sulfuric acid in air.[1] However, there is an increasing body of experimental evidence that some gases may also undergo unique reactions at the air–water interface. In one of the first papers proposing this possibility, Jayne *et al.*[2] reported that the uptake of SO_2 into aqueous droplets could not be described without including a surface reaction involving an SO_2 complex at the interface; the conversion of this surface complex into H^+ and HSO_3^- was proposed to determine the rate of uptake of SO_2. Donaldson and coworkers[3,4] subsequently reported spectroscopic detection of an SO_2 surface complex in second harmonic generation spectroscopic studies of gas evolving from $NaHSO_3$ solutions. There was also a large reduction in the surface tension of these solutions and a saturation surface coverage of 5×10^{14} cm^{-2} of an uncharged SO_2 surface complex was proposed. Additional examples of reactions of gases such as Cl_2, Br_2, $ClNO_2$, $ClONO_2$ and OH with ions at the air–water or sulfuric acid solution interfaces, possibly *via* the formation of initial surface complexes, were subsequently reported,[5–8] highlighting the importance of understanding the nature of such complexes at the air–water interface.

Boniface *et al.*[9] reexamined the uptake and reactions of SO_2 in water and found that SO_2 reacts rapidly with OH^-; the enhanced uptake observed in the earlier studies[2] at pH > 10 was shown to be due to this previously unrecognized reaction. However, a one-time uptake of SO_2 at pH < 2 was still observed and attributed to the formation of an SO_2 surface complex, with the number of available surface sites for SO_2 uptake being ~10^{14} SO_2 cm^{-2} as reported in the earlier studies.[2] Clegg and Abbatt[10] recently reported the uptake of gaseous SO_2 on ice surfaces at temperatures from 213 to 238 K. The measured uptake of SO_2 was observed to be consistent with the Jayne *et al.*[2] model, where the interfacial form of SO_2 [shown below as SO_2(interface)] involves interaction with a few water molecules at the surface, and the subsequent conversion to an ionic form determines the uptake:

$$SO_2(g) \leftrightarrow SO_2(interface) \quad (1)$$

$$SO_2(interface) \leftrightarrow (H^+/HSO_3^-)(interface) \quad (2)$$

Infrared spectroscopic measurements could be very useful in probing for the existence and nature of such interfacial species, and hence providing insight into its unique reactions at the interface. It can be inferred from the *ab initio* calculations by Bishenden and Donaldson[11] on the 1:1 SO_2:H_2O gas phase complex that there may be a red shift of ~25 cm^{-1} in the ν_3

† Present address: Department of Chemistry, University of Idaho, Moscow, ID 83844-2343, USA
‡ Present address: SensIR Technologies, 15 Great Pasture Road, Danbury, CT 06810-9931, USA
§ Correspondence for theoretical calculations and experiments should be addressed to RBG (E-mail: bgerber@uci.edu) and BJFP (E-mail: bjfinlay@uci.edu; Fax: (949) 824-3168; Tel: (949) 824-7670), respectively.

 DOI: 10.1039/b108907b

asymmetric stretch of SO_2 on binding to water relative to the gas phase absorption, which occurs at 1361 cm^{-1}. One experimental approach for observing such a shifted absorption is the use of sum frequency generation (SFG) spectroscopic measurements which probes only the interface;[12–15] however, covering the full range of infrared frequencies of interest is often not possible. Another approach is the use of single reflectance (SR) infrared spectroscopy which has been applied, for example, to monolayers of phospholipids at the air–water interface.[16–22] This technique has the advantage that a wide range of infrared frequencies are measured. However, the infrared beam penetrates beyond the interface region into the bulk to a depth of the order of a few microns, depending on the frequency of the radiation and nature of the liquid; thus it probes the surface film, rather than just the interfacial region. As a result, if there are significant concentrations of dissolved compounds in addition to interfacial species, it can be difficult to separate the contributions of the interface species.

An alternate approach is attenuated total reflectance (ATR) combined with FTIR. ATR is an internal reflection technique in which light is directed into an infrared transmitting crystal. It strikes the interface at an angle greater than the critical angle and hence undergoes total internal reflection.[23] There is an evanescent wave that penetrates into the surrounding medium, with the depth of penetration depending on the angle of incidence and the indices of refraction of the crystal and the surrounding medium; typical depths of penetration are of the order of a few microns.[23] As a result, if single beam spectra with and without the absorbing species are ratioed, an absorption spectrum of infrared active species in the medium surrounding the crystal can be obtained. If the species adsorbs directly onto the crystal itself, it would also be detected. Such cells are normally used with liquids, and have proven particularly advantageous with aqueous solutions since the net pathlength through the absorbing water solvent is minimized. ATR has also been used extensively with solids and their interactions with gases[24] and liquids.[25,26] Horn and Sully[27,28] applied ATR to study the uptake of gases onto ice surfaces[27] as well as the formation of sulfuric acid–water films when SO_3 and H_2O were co-condensed on a Ge crystal at $T \leqslant 250$ K. Thus, ATR has been demonstrated to be a highly useful technique for studying both bulk materials and thin films.

As a result, we have chosen this technique to study the chemistry in these water films at room temperature. Thin films of water can be formed on the ATR crystal by exposure to water vapor, and the thickness of the film can be determined from the water absorption bands. In this case, even though the evanescent wave probes on the order of a micron away from the interface, the absorbing film is <30 nm in depth and determines the infrared absorption spectrum. If interfacial species are formed at the air–water interface in sufficient concentrations, they should also be detectable, since this small film thickness maximizes contributions to the infrared absorption by interfacial compared to dissolved species.

We report here a search for the previously proposed uncharged SO_2–water complex in surface films of water solutions using attenuated total reflectance Fourier transform infrared spectroscopy (ATR-FTIR). For comparison, we have obtained transmission and single reflectance spectra of saturated aqueous solutions of SO_2. To assist in our search for a complex, we have also carried out electronic structure calculations on the SO_2–H_2O complex in the gas phase, both for the lowest energy configuration (which has a 'sandwich' type structure) and for a hydrogen-bonded structure of slightly higher (1.6 kcal mol^{-1}) energy (see Fig. 1). The combination of these approaches allows us to put an upper limit on the concentration of an SO_2–water surface complex at the air–water interface of 4×10^{14} SO_2 cm^{-2}, based on the experimental data and assuming its structure can be represented by a 1:1 SO_2–H_2O or similar complex.

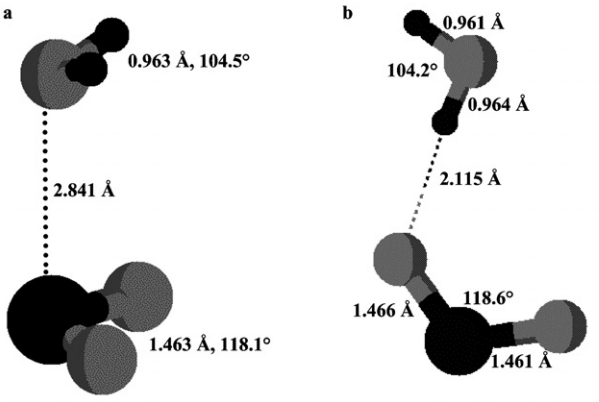

Fig. 1 Geometry of (a) the lowest energy and (b) a hydrogen-bonded configuration of the SO_2–H_2O complex, calculated at the MP2/aug-cc-pvtz level.

Experimental

Measurements using attenuated total reflectance

Experiments were carried out using two types of ATR probes: a fiber optic probe (Thermo Spectra-Tech, ATR Needle Probe) and a Tunnel cell® (Axiom Analytical, Inc., Irvine, CA). Most of the experiments reported here were carried out with the fiber optic probe that consisted of an infrared-transmitting chalcogenide (AsSeTe) fiber embedded in an epoxy support and polished to expose a portion of the fiber; the number of reflections is three. From the angle of incidence ($\theta = 45°$) and the refractive index of chalcogenide ($n_1 = 2.8$), the depth of penetration (d_p) of the evanescent wave can be calculated[23] from $d_p = \lambda/[2\pi n_1(\sin^2\theta - n_{21}^2)^{1/2}]$, where $n_{21} = n_2/n_1$ and n_2 is the index of refraction of the rarer medium surrounding the crystal. At 3400 cm^{-1}, d_p is 0.28 μm for air and 0.32 μm for water; at 1150 cm^{-1}, the corresponding values are 0.82 μm (air) and 0.94 μm (water), respectively. As discussed in detail later, the depth of penetration of the beam is much larger than the thickness of the water films deposited on the crystal. As a result, the evanescent wave probes not only the species dissolved in the film, but also any surface-adsorbed species present. In addition, for such thin films, the effective thickness, d_e, of the film and hence the relative intensities do not depend on wavelength, resulting in spectra that are very similar to transmission spectra (this is not the case for bulk materials, where the effective thickness depends on wavelength).[23]

The probe was mounted in a borosilicate glass cell so that the infrared fiber could be exposed to gases in the cell under controlled conditions. The cell was attached to a conventional vacuum system for introducing gases, and to a 50 mL bulb containing water (Barnstead, Nanopure) which had been through a freeze–pump–thaw cycle. The probe was mated to a Mattson RS Series FTIR using a "Foundation" transfer optic (Thermo Spectra-Tech) located in the sample compartment.

After the cell was pumped out, it was allowed to come to equilibrium with the water in the bulb. The water vapor pressure was not measured directly, but some condensation on the cell walls was observed visually. The presence of a thin water film led to a strong absorption at ~3400 cm^{-1} that is characteristic of liquid water (ν_1).[29] Gaseous SO_2 (Matheson, Anhydrous) was then introduced into the cell to a measured total pressure and the single beam spectrum recorded. For comparison, a spectrum was also recorded with SO_2 added to the cell

in the absence of water vapor. In each case, a total of 1000 scans at 4 cm^{-1} resolution was used with the cell sealed off, *i.e.* in the static mode.

The thickness of the water film on the fiber optic surface was quantified in the following manner.[23] The reflectivity, R^N, for N reflections and weak absorptions is given by

$$R^{N} \cong 1 - N\alpha d_e \quad \text{(I)}$$

where d_e is the effective thickness, a parameter which reflects the coupling between the evanescent wave and the sample, and which can be related to the corresponding transmission spectrum for which $I/I_0 = e^{-\alpha l}$ where l is the pathlength. The absorption parameter, a, is given by

$$a = (1 - R^{N}) \cong N\alpha d_e \quad \text{(II)}$$

and is measured in these experiments by measuring the reflectivity as the ratio of the single beam spectrum in the presence of the sample to that in the absence of the water film. (For ease of presentation, spectra are shown as absorbance ($\log I_0/I$) *versus* wavenumber.) Rather than using the intensity at one wavenumber, the band was integrated over the wavelength region 2800–3800 cm^{-1} and the optical constants from Bertie and Lan[30] applied to obtain the effective thickness, d_e. Taking 0.35 nm as the depth of one monolayer of water, the number of water layers was calculated as $d_e/0.35$. In these experiments, the water layers were sufficiently thick that the infrared spectrum was indistinguishable from that of bulk liquid water, in contrast to the case of 1–5 water layers where the spectrum shows that the water is significantly perturbed by the underlying surface.[31] Therefore, application of the optical constants for liquid water are appropriate in the present experiments.

A second type of ATR experiment was carried out using the Tunnel cell® that consists of an $1/8''$ infrared-transmitting AMTIR (GeAsSe) crystal of length $1.5''$ situated in a cylindrical sample holder. For this particular cell, approximately 10 such internal reflections occur along the length of the rod. The cell was located in the sample compartment of a Mattson Galaxy FTIR spectrometer (Model 5020). The thin liquid water film was first formed on the crystal by flowing a stream of N_2 containing H_2O vapor at a given relative humidity and a total pressure of 1 atm through the cell. Some of the vapor condensed on the crystal, forming a thin film of liquid water which was again quantified using the liquid water infrared absorption at ~3400 cm^{-1}. Gaseous SO_2 at approximately 1 atm pressure was then introduced into the cell and the spectrum recorded, again in the static mode. Comparison spectra using SO_2 in the absence of water were also measured. For these experiments, 1024 scans at 0.5 cm^{-1} resolution were recorded.

Measurement of transmission and single-reflectance FTIR spectra

For comparison to the ATR spectra, we also measured transmission spectra of the corresponding solutions. The transmission cell (McCarthy Scientific Co.) had CaF_2 windows and a 50 μm Teflon spacer. Spectra of water saturated with SO_2 and of $NaHSO_3$ (Fisher Scientific Certified ACS grade) were recorded at a resolution of 0.5 cm^{-1} and using a total of 1024 scans.

SR-FTIR spectra of saturated $NaHSO_3$ and SO_2 saturated water were measured in an apparatus similar to the one described previously[32] but with a closed sample cell to prevent loss of gases. The infrared beam passed through a CaF_2 window to the surface where it is reflected by the liquid back through the CaF_2 window to an MCT detector. The resolution used for these studies was typically 0.5 cm^{-1}. Although lower resolution could have been used for the surface and bulk phase species, use of 0.5 cm^{-1} resolution optimized the identification and subtraction of gas phase SO_2 from the spectra. A warm stream of nitrogen gas flow was directed onto the outside of the CaF_2 window in order to prevent condensation of water on the inside of the window; uptake of water or SO_2 into water films on the window was detectable in the single reflectance spectrum as positive absorbance signals superimposed on the differential-shaped peaks due to the bulk species, and because this complicated the data analysis, it was avoided.

Infrared reflectance spectra of bulk solutions contain contributions from species in the gas phase, in the top few microns of the liquid phase, and when present at sufficient concentrations, at the interface. The absorption bands for gas-phase species are similar to the peaks observed in a normal transmission spectrum, and were removed by subtracting an appropriate gas-phase reference spectrum. Reference spectra of SO_2 were taken in the same cell by introducing the gas into the cell and replacing the liquid solution with a reflecting mirror coated with gold and a protective overlayer of silicon monoxide. Although SO_2 has been observed to adsorb on gold[33] it is not known to adsorb on glass surfaces at room temperature and hence would not be expected to do so on the silicon monoxide coated mirror. The SR spectra were analyzed as described in earlier studies[32] using the Kramers–Kronig (KK) transform[34,35] to obtain the absorption coefficient (k) spectrum as a function of wavenumber.

In single reflectance spectra, the absorption bands responsible for the species in the bulk liquid appear as differential-shaped peaks. The Kramers–Kronig (KK) transform[34,35] converts the reflectance spectrum into an absorption spectrum with positive bands similar to those obtained using transmission. If there is an interfacial layer between air and the bulk aqueous solution, the absorption bands for these species appear as negative peaks,[16,18,19] and become differential in shape after application of the KK transform.

All measurements were carried out at 298 ± 2 K.

Results and discussion

Ab initio calculations

Calculations by Bishenden and Donaldson[11] suggest that the ν_3 asymmetric stretch for gas phase SO_2 at 1361 cm^{-1} may red-shift by as much as 25 cm^{-1} when SO_2 is complexed to one water molecule. To provide further guidance for our experiments, *ab initio* calculations were carried out for gaseous SO_2 as well as a 1:1 SO_2:H_2O complex in the two configurations shown in Fig. 1. Fig. 1a is a 'sandwich' type structure and Fig. 1b is a hydrogen-bonded structure of slightly higher (1.6 kcal mol^{-1}) energy.

Table 1 compares our calculated harmonic frequencies for gas phase SO_2 and for both structures of the SO_2–H_2O complex. All calculations were performed with the Gaussian 94 electronic structure[36] package at the MP2/aug-cc-pvtz level of theory. The agreement between the experimental frequencies and those calculated at this level of theory for SO_2(g) is good, and certainly sufficient to give us confidence in the theoretical method used. Blue shifts of 3 to 12 cm^{-1} are calculated when gas phase SO_2 forms the lowest energy 1:1 "sandwich" complex with water shown in Fig. 1a. No significant differences in the relative band intensities are predicted for the complex compared to SO_2 itself. As discussed below, shifts for complexes of SO_2 with more than one water molecule but less than the bulk would be expected to fall between these two extremes; the calculations on the 1:1 complex and measurements of the spectrum in the bulk allow one to focus the experiments accordingly.

Interactions between SO_2 and water are weak compared to those between water molecules, which form a strong hydrogen-bonded network at the air–water interface, with some dan-

Table 1 Comparison of calculated frequencies (cm^{-1}) for gas phase SO_2 and its 1:1 complex with water

Species	Vibrational modes (experimental gas phase frequencies)[a]	Calculated frequencies MP2/aug-cc-pvtz		Experimental frequencies (Ar matrix)[44,45]	Calculated frequencies MP2/6-31G(d)	Calculated frequencies MP2/6-31 + G(d,p)
SO_2	ν_2 bend (519)	493.4		517.2	486.4[d]	478.9
	ν_1 sym. str. (1151)	1099.5		1147.1	1077.5[d]	1060.0
	ν_3 asym. str. (1361)	1305.7		1351.1	1305.5[d]	1271.6
SO_2–H_2O (shift from SO_2)	ν_2 bend	500.7 (+7.3)[b]	495.6 (+2.2)[c]	521.8 (+4.6)	497.9 (+11.5)	487.0[d] (+8.1)
	ν_1 sym. str.	1111.8 (+12.3)[b]	1101.6 (+2.1)[c]	1150.0 (+2.9)	1099.2 (+21.7)	1077.4[d] (+17.4)
	ν_3 asym. str.	1308.8 (+3.1)[b]	1303.9 (−1.8)[c]	1343.3 (−7.8)	1316.7 (+11.2)	1280.8[d] (+9.2)

[a] From ref. 46. [b] For the 'sandwich' structure in Fig. 1a. [c] For the hydrogen-bonded structure in Fig. 1b. [d] From ref. 11.

gling O–H bonds projecting into the gas phase.[37–43] Given the presence of the dangling OH at the interface, one might expect intuitively that a configuration with the H_2O hydrogen-bonded to the SO_2 might exist and play a significant role. We therefore also examined the hydrogen-bonded configuration of SO_2–H_2O shown in Fig. 1b that we found to be a local minimum on the potential energy surface. This structure was found to be approximately 1.6 kcal mol^{-1} higher in energy than the structure shown in Fig. 1a and, as Fig. 1b shows, neither the O–H nor the S–O bond lengths are influenced significantly by the hydrogen bond. The harmonic frequencies for this structure are shown in Table 1 and they show ~2 cm^{-1} red shift in the asymmetric stretching ν_3 mode, and blue shifts in the ν_1 symmetric stretch and ν_2 bending modes, also of ~2 cm^{-1}. Thus, the weak interactions between SO_2 and H_2O in the 1 : 1 complex in the gas phase do not induce large changes in the fundamental frequencies of SO_2 for either of the two structures shown in Fig. 1.

Also shown in Table 1 for comparison to the calculations are experimentally measured values for SO_2 and for the SO_2–H_2O complex in an argon matrix at 17–19 K.[44,45] Assuming the shift due to the argon matrix is the same for SO_2 and SO_2–H_2O, the experimentally determined blue shifts are 3–5 cm^{-1} for the ν_1 and ν_2 bands at 1147 and 517 cm^{-1}, respectively, with a red-shift of 8 cm^{-1} for the ν_3 band at 1351 cm^{-1}. The lack of exact quantitative agreement between theory and experiment regarding the absolute magnitude of the shifts is due to several factors. On the theoretical side, the level of electronic structure theory and the harmonic approximation that was used to calculate the frequencies both contribute to the uncertainties in the predicted frequency shifts upon complexation with water. On the experimental side, the interaction with the Ar matrix may modify the structure of the SO_2–H_2O complex slightly when compared to the gas phase.

The calculations by Bishenden and Donaldson[11] were carried out for the SO_2–H_2O complex in its minimum energy "sandwich" configuration. From their summary of vibrational constants in Table 2 of that paper, almost no shifts in the ν_2 and ν_1 modes, and a red-shift of 25 cm^{-1} in the ν_3 mode, of SO_2 can be inferred. The vibrational constants they cite are based on a calculation for the SO_2 monomer using a MP2/6-31G(d) level of theory and for the complex, using MP2/6-31+G(d,p). However, the slightly larger basis set used on the complex when compared to the monomer means that these should not be used for a direct calculation of the shifts in frequencies for SO_2 expected on binding to water. For a more direct comparison, we have also carried out calculations for SO_2 at the MP2/6-31+G(d,p) level of theory and for the 1:1 SO_2:H_2O complex using MP2/6-31G(d,p). As shown in Table 1, if the comparison between the monomer and the complex is performed using the *same* basis set, then a blue shift in all the modes of ~8–22 cm^{-1} is predicted with both the 6-31G(d) and 6-31G+(d,p) basis sets. The results in Table 1 suggest that the shift of the ν_3 mode reported in ref. 11 may be somewhat overestimated due to the use of different basis sets for the complex and for isolated SO_2. However, the discrepancy between the two sets of calculations is not large, and both imply the complexation shift in the 1:1 SO_2:H_2O gas phase complex in its equilibrium geometry is relatively small.

Although the absolute values of the fundamental frequencies are quite different when calculated using the three different basis sets, the values of the shifts are all very similar. If one assumes that the errors in the calculated frequencies are the same for both SO_2 and SO_2:H_2O, then this behaviour is to be expected and allows us to have much more confidence in the shifts we predict than the absolute values of the frequencies.

Infrared spectra of dissolved sulfur dioxide

In aqueous solution, the SO_2 molecule will interact with a number of water molecules simultaneously. Fig. 2 shows infrared spectra of aqueous solutions generated by bubbling SO_2 through water to form a saturated solution. Fig. 2a is the measured reflectance spectrum which shows a strong positive peak at 1361 cm^{-1} and weak peak at 1151 cm^{-1} due to gaseous SO_2 above the solution, as well as weaker peaks due to solution phase species. Fig. 2b shows the same spectrum after subtraction of gas phase SO_2 and Fig. 2c the spectrum after application of the KK transform to the spectrum in Fig. 2b. Positive peaks at 1330 and 1152 cm^{-1} are observed in Fig.

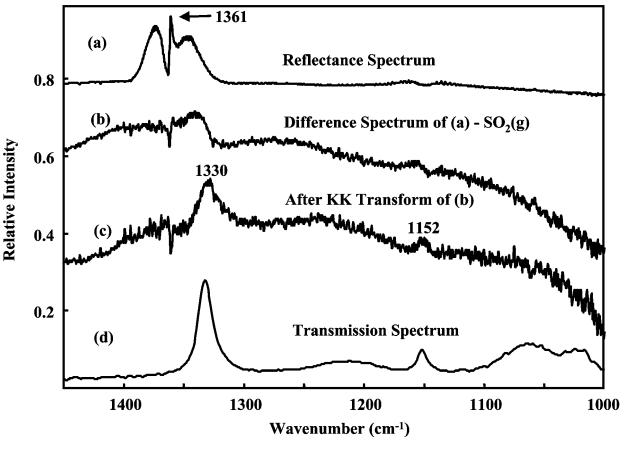

Fig. 2 Single reflectance spectra of water saturated with SO_2 (a) as measured; (b) after subtraction of the contribution due to gas phase SO_2; (c) after application of the Kramers–Kronig transform. The equilibrium concentrations in the aqueous phase are calculated to be 1.2 M SO_2(aq), 0.13 M HSO_3^- and 1×10^{-3} M $S_2O_5^{2-}$ and a pH of 0.9; (d) transmission spectrum of an SO_2–saturated water solution which has been diluted by a factor of 10. The equilibrium concentrations are calculated to be 0.1 M SO_2(aq), 0.04 M HSO_3^- and 1×10^{-4} M $S_2O_5^{2-}$, with a pH of 1.4.

2c, indicating they are due to a species present in the top layer of the bulk solution. The same peaks are also present in a transmission spectrum of a similar solution that has been diluted by a factor of 10 (Fig. 2d), and are characteristic of the ν_3 and ν_1 modes of SO_2 in water, respectively.[47,48] Also seen in Fig. 2d are weak, broad peaks at 1028 cm^{-1} due to HSO_3^- in equilibrium with SO_2(aq) and at ~1060 cm^{-1} from $S_2O_5^{2-}$ in equilibrium with 2 HSO_3^-.[48,49] From the known equilibrium constants,[1,50,51] the concentrations for the solution in Fig. 2d are calculated to be 0.1 M SO_2(aq), 0.04 M HSO_3^- and 1×10^{-4} M $S_2O_5^{2-}$, with a pH of 1.4. As discussed in detail elsewhere,[47,50] SO_2 is not strongly hydrated in aqueous solution so that its infrared spectrum is similar to that of liquid SO_2.[52] There was no evidence of differential-shaped peaks after application of the Kramers–Kronig transform, indicating that interfacial species, if they exist, were present at concentrations too small to be observable in these experiments.

The spectra in Fig. 2 clearly show the shift in the ν_3 asymmetric stretch from 1361 cm^{-1} for gas phase SO_2 to 1330 cm^{-1} when the SO_2 is surrounded by a number of water molecules in aqueous solution. The blue shift in the ν_1 symmetric stretch is small, several wavenumbers or less. Due to the different geometry and the smaller number of water molecules in contact with SO_2 for a surface complex, the vibrational shifts for surface-adsorbed SO_2 are likely to be smaller in magnitude than for SO_2 in bulk liquid water.

Thus, based on our theoretical calculations (Table 1), the experimentally observed shifts in argon matrices,[44,45] and the position of this band in aqueous solution (Fig. 2), it is reasonable to expect the ν_1 symmetric stretch for the SO_2 surface complex with water will be within several wavenumbers of 1151 cm^{-1}. Because the corresponding absorptions of aqueous sulfur species are at 1152 cm^{-1} and are broad, a unique signal due to the surface species will be difficult to detect in this region. However, the combination of the theory and experimental data suggest that the ν_3 asymmetric stretch which appears at 1361 cm^{-1} for gaseous SO_2(g) will be shifted by ~2–8 cm^{-1} for a surface species interacting with one water molecule. Presumably interactions with more than one water molecule, but less than the number in the bulk solution, will lead to shifts that are greater than 8 cm^{-1} but less than the 31 cm^{-1} for SO_2(aq). This is supported by the matrix infrared studies of Schriver *et al.*[45] who reported absorption bands not only for the 1:1 complex (Table 1) but also for the 2:1 H_2O–SO_2 complex. Compared to SO_2 in an Ar matrix,[44] the ν_3 asymmetric stretch of the 2:1 H_2O–SO_2 complex was red-shifted by 12 cm^{-1}, and the ν_1 was blue-shifted by 10 cm^{-1}, larger in both cases than for the 1:1 complex.

If the absorption band for the SO_2 surface complex was very broad, it would be difficult to detect. However, this is not likely to be the case. The width of the SO_2(aq) absorption band reflects a time-averaged set of changing interactions of SO_2 with a number of different water molecules. The surface complex is expected to interact simultaneously with fewer water molecules, on average, than SO_2(aq) in the bulk. The width of the absorption band for the surface complex, which reflects in part these changing interactions with water, would therefore not be expected to be significantly different than that of SO_2(aq). Because the gas phase does not contribute a measurable signal in ATR due to the small depth of penetration of the evanescent wave, and the absorption due to SO_2(aq) is shifted by 31 cm^{-1}, we expect that a signal from the shifted ν_3 asymmetric stretch of a surface SO_2 complex should be observable in our experiments.

ATR infrared experiments

To probe experimentally for the existence of a surface complex using ATR-FTIR, spectra were obtained using the fiber optic probe when SO_2 was present at ~1 atm pressure in the absence of water and then in its presence. Fig. 3a shows the spectrum obtained in the absence of water vapor. Weak peaks at 1330 and 1145 cm^{-1} are seen. Since there is little water present on the crystal under these conditions as evidenced by the absence of the strong band around 3400 cm^{-1}, these peaks must be due to SO_2 physisorbed on the crystal surface. The nature of physisorbed SO_2 is not clear, but the band positions are similar to those reported for liquid SO_2,[52] 1338 and 1148 cm^{-1}, and gas phase clusters and thin film SO_2 at low temperatures,[53] ~1330 and ~1140 cm^{-1}. One possibility is that SO_2 exists on the surface in 2D "islands" involving SO_2–SO_2 interactions, similar to that reported for water at low coverages on salt[54,55] and on borosilicate glass surfaces.[31]

Fig. 3b shows the spectrum when a similar pressure of SO_2 was added to the cell which had been allowed to equilibrate first with the bulb of liquid water. Peaks due to liquid water at ~3400 and 1640 cm^{-1} are present. The peak at 1330 cm^{-1} has increased in intensity, and the 1145 cm^{-1} peak has broadened and shifted slightly to 1147 cm^{-1}.

With water present, gaseous SO_2 will dissolve to form SO_2(aq), HSO_3^- and SO_3^{2-} in the thin water film on the ATR crystal surface. From the 3400 cm^{-1} liquid water band, the effective thickness (d_e) of the water film is estimated as described above to be 2.8×10^{-6} cm, corresponding to 80 monolayers of water. From the known equilibria and kinetics in water,[1,50,51] equilibrium with gaseous SO_2 should be rapidly attained, with SO_2(aq) and HSO_3^- as the major sulfur species present in the water film. For the conditions of Fig. 3b, the concentrations of SO_2(aq) and HSO_3^- are calculated to be 1.05 M and 0.12 M respectively, and the pH is calculated to be 0.9. The increase in the 1330 cm^{-1} peak in the presence of water is therefore likely to be due to SO_2(aq) whose major absorption peak is at 1330 cm^{-1} (Fig. 2).[52]

Fig. 4 shows an expanded region from 1400 to 1100 cm^{-1} for the experiment in Fig. 3b. Fig. 4a shows the difference between the spectrum with both SO_2 and water present and that when water was present alone before SO_2 was added. Fig. 4b shows the spectrum of SO_2 in the absence of water. Fig. 4c is the difference between Fig. 4a and 4b, showing the new bands that are formed when both water and SO_2 are present compared to SO_2 or water alone. Peaks at both 1330 and 1152 cm^{-1} are seen, as expected for SO_2(aq). Furthermore, they are in the same ratio, within experimental error, of those measured in the transmission and single reflectance spectra (Fig. 2c and d). Thus, when both water and SO_2 are present, SO_2(aq) is formed in the thin water film on the crystal surface, as expected.

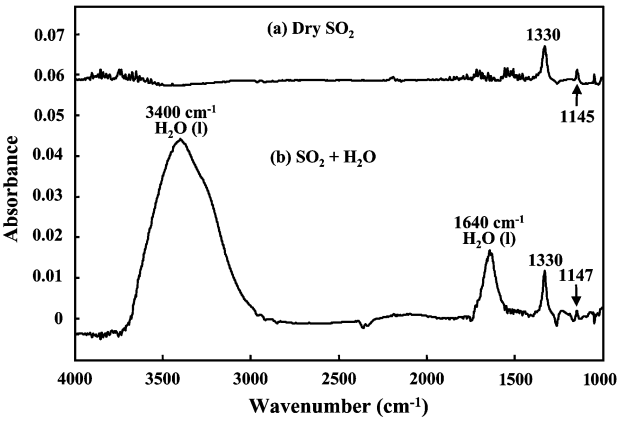

Fig. 3 ATR spectra in the presence of (a) 630 Torr SO_2(g) and (b) 645 Torr SO_2 added to the cell after the crystal had come to equilibrium with ~24 Torr water vapor, forming a thin water film on the crystal. The equilibrium concentrations are calculated to be 1.05 M SO_2(aq), 0.12 M HSO_3^- and 1×10^{-3} M $S_2O_5^{2-}$, with a pH of 0.9.

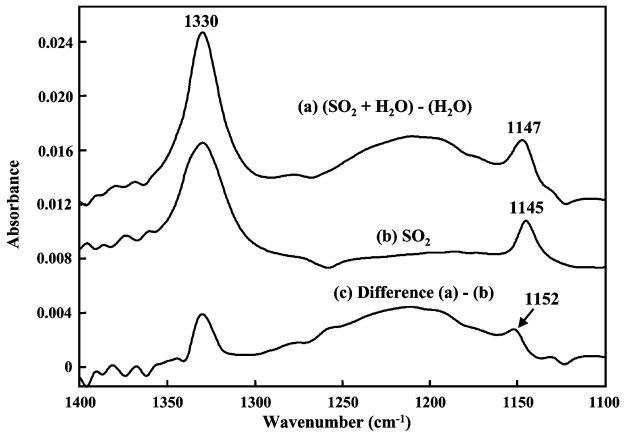

Fig. 4 Expanded region for experiment described in Fig. 3. (a) Spectrum in Fig. 3b after subtraction of the spectrum of water alone before the addition of gaseous SO_2; (b) spectrum of SO_2 alone as shown in Fig. 3a; (c) difference spectrum 4a − 4b. The broad feature between the two SO_2 peaks at 1330 and 1152 cm^{-1} is likely to be due to small baseline shifts which are also manifested as similar broad features in other regions of the spectrum.

The fact that a peak remains at 1145 cm^{-1} when water is added to the cell suggests that even in the presence of water, some SO_2 continues to interact with the surface in a manner similar to the dry case, in addition to dissolved sulfur oxide species being formed in the water film. A question arises as to whether the 1330 and 1145 cm^{-1} bands observed in the presence of water could be assigned to an SO_2 complex of water at the interface. This seems unlikely since the shift of ~30 cm^{-1} from 1361 to 1330 cm^{-1} appears to be characteristic of condensed phases or clusters where the SO_2 is surrounded by other SO_2 or water molecules. At the interface, SO_2 will not be surrounded in such 3D structures and hence, as our calculations and the matrix isolation experiments[44,45] show, such a large shift is not expected for the surface complex.

With a water film of thickness 2.8×10^{-6} cm, the volume of water over a 1 cm^2 area of the crystal surface is 2.8×10^{-9} L. Given a concentration of SO_2(aq) of 1.05 M, there are 2×10^{15} SO_2 molecules per cm^2 dissolved in the water film and these give the increase in absorbance of 0.0046. Our detection limit of 0.001 (based on three times the peak-to-peak noise in this region) therefore corresponds to $\sim 4 \times 10^{14}$ cm^{-2} for SO_2(aq). A second set of similar experiments gave a detection limit of 3×10^{14} cm^{-2}. If the surface complex of SO_2 has a similar absorption coefficient, then it therefore should be detectable at levels $\geqslant 4 \times 10^{14}$ cm^{-2} in these experiments. We believe that this is a conservative estimate, in that the 1152 cm^{-1} peak due to SO_2(aq) in Fig. 4c has a peak absorbance above the baseline of 0.001, equivalent to our stated detection limit, but is very clearly visible in the spectrum.

A careful examination of ATR spectra such as those in Fig. 4 revealed no new bands that were not attributable to SO_2(aq) or physisorbed SO_2. There are no new bands between 1361 cm^{-1} where gas phase SO_2 absorbs and 1350 cm^{-1}, the region where the combination of calculations and matrix experiments suggest a 1:1 surface complex of SO_2:H_2O should be observable. (The small peaks seen in the spectra in the 1400 to 1360 cm^{-1} region are due to incomplete subtraction of gas phase water due to changes in the purging of the sample compartment of the spectrometer.) Thus, this surface complex of SO_2, if it exists, must be present at less than 4×10^{14} cm^{-2}. It is reasonable to expect that if it interacted with several water molecules, it might be further red-shifted below 1350 cm^{-1}; for example, the low temperature matrix studies[44,45] suggest that the interaction with two water molecules would red-shift the band by 12 cm^{-1}. Because of the tail of the SO_2(aq) band at 1330 cm^{-1}, this would be more difficult to observe but again, no detectable peaks are observed in this region.

Experiments were also carried out using the 10-reflection Tunnel cell® designed for use with liquid solutions. The results were essentially identical. That is, peaks at 1330 and 1145 cm^{-1} were observed with SO_2 in the absence of water, with the 1330 cm^{-1} peak being enhanced in the presence of water by an amount consistent with the formation of SO_2(aq) in the thin water film. In this case, the water film was only 18 monolayers thick so that the amount of SO_2(aq) on the crystal surface was significantly less than for the experiment shown in Fig. 3 using the needle probe, and the 1152 cm^{-1} peak was not observable. Analysis similar to that described above gives an upper limit to the 1:1 SO_2:H_2O surface complex of 2×10^{14} cm^{-2}, but this is considered to be less reliable because of the need to subtract a contribution from small amounts of gas phase SO_2 present in the light path in the sampling compartment due to leakage from the cell. However, it is noteworthy that in all respects the results were the same when a different ATR crystal and experimental system was used, ruling out unrecognized artifacts from a particular crystal surface.

Boniface *et al.*[56] observed a one-time uptake of SO_2 onto aqueous solutions at pH < 2, which based on the data of Jayne *et al.*,[2] corresponds to a saturation concentration of surface sites of $\sim 10^{14}$ cm^{-2}; a surface complex at this concentration would not have been observable in our experiments. Donaldson *et al.*[3] estimated a saturation surface coverage of 5×10^{14} SO_2 per cm^2 in their SHG and surface tension measurements of gases evolving from $NaHSO_3$ solutions, and proposed that this was due to an uncharged SO_2 surface complex. While this is only slightly larger than our detection limit, it seems likely from Fig. 4 that if an uncharged 1:1 SO_2 surface complex were present in our experiments at this concentration, it would have been observable.

Several groups[2,10,51] have proposed that the uptake of SO_2 into water or ice occurs by the formation of a surface SO_2 complex that then dissociates into surface ionic species (eqns. (1) and (2) above). The expected absorption bands for such an ionic complex are not known but one might expect that they would be in the region of the HSO_3^- absorption bands. The weak, broad peak around 1028 cm^{-1} in Fig. 2d is due to HSO_3^-.[48,49] From this spectrum, the molar extinction coefficient at 1028 cm^{-1} is estimated to be 2.8×10^2 M^{-1} cm^{-1}, about half that for the 1330 cm^{-1} band of SO_2(aq). If a surface HSO_3^- exists and has an absorption coefficient similar to that for HSO_3^-(aq), our detection limit for the surface species would be about twice that for SO_2(aq), or $\sim 8 \times 10^{14}$ cm^{-2}.

In summary, no new peaks or significant shifts in sulfur dioxide peaks normally found in aqueous solutions were observed in any of the experiments, from which an upper limit to the concentration of a 1:1 SO_2–water or similar complex at the air–water interface of 4×10^{14} cm^{-2} can be estimated.

Conclusions

Attenuated total reflectance Fourier transform spectrometry provides a powerful means of searching for surface complexes using well-developed and readily available spectroscopic methods. The inorganic species for which there is the greatest evidence from previous studies for the formation of a surface complex at the air–water interface is SO_2, which is hypothesized to convert to an ionic form at the surface. A search for a 1:1 or similar neutral complex of SO_2 with water at the surface of aqueous solutions using this approach did not reveal any absorption bands attributable to such an interfacial species, from which concentrations higher than 4×10^{14} complexes cm^{-2} can be excluded with some confidence. Understanding the molecular form of this complex, if it exists,

is important for elucidating its role in the physical and chemical properties of the interface of aqueous solutions in the presence of SO_2, such as the reported reduction in surface tension. Future searches to elucidate the nature of this surface species need to be capable of detecting surface concentrations of the order of 10^{14} cm^{-2} or less.

Acknowledgement

We are grateful to the California Air Resources Board for support of this work. We also thank P. R. Griffiths, R. A. Dluhy, D. J. Donaldson, C. Higgins, C. E. Kolb, D. R. Worsnop and P. Davidovits, S. Fleming and M. Doyle for helpful discussions, and D. J. Donaldson for providing a preprint prior to publication. This research was also supported in part by a grant from the Petroleum Research Fund administered by the American Chemical Society.

References

1 B. J. Finlayson-Pitts and J. N. Pitts, *Chemistry of the Upper and Lower Atmosphere: Theory, Experiments and Applications*, Academic Press, San Diego, 2000.
2 J. T. Jayne, P. Davidovits, D. R. Worsnop, M. S. Zahniser and C. E. Kolb, *J. Phys. Chem.*, 1990, **94**, 6041.
3 D. J. Donaldson, J. A. Guest and M. C. Goh, *J. Phys. Chem.*, 1995, **99**, 9313.
4 S. Izmailova, E. Bishenden and D. J. Donaldson, submitted for publication.
5 D. R. Hanson and A. R. Ravishankara, *J. Phys. Chem.*, 1994, **98**, 5728.
6 J. H. Hu, Q. Shi, P. Davidovits, D. R. Worsnop, M. S. Zahniser and C. E. Kolb, *J. Phys. Chem.*, 1995, **99**, 8768.
7 C. George, W. Behnke, V. Scheer, C. Zetzsch, L. Magi, J. L. Ponche and P. Mirabel, *Geophys. Res. Lett.*, 1995, **22**, 1505.
8 E. M. Knipping, M. J. Lakin, K. L. Foster, P. Jungwirth, D. J. Tobias, R. B. Gerber, D. Dabdub and B. J. Finlayson-Pitts, *Science*, 2000, **288**, 301.
9 J. Boniface, Q. Shi, Y. Q. Li, J. L. Cheung, O. V. Rattigan, P. Davidovits, D. R. Worsnop, J. T. Jayne and C. E. Kolb, *J. Phys. Chem. A*, 2000, **104**, 7502.
10 S. M. Clegg and J. P. D. Abbatt, *J. Phys. Chem. A*, 2001, **105**, 6630.
11 E. Bishenden and D. J. Donaldson, *J. Phys. Chem. A*, 1998, **102**, 4638.
12 K. B. Eisenthal, *Annu. Rev. Phys. Chem.*, 1992, **43**, 627.
13 K. B. Eisenthal, *Acc. Chem. Res.*, 1993, **26**, 636.
14 Y. R. Shen, *Annu. Rev. Phys. Chem.*, 1989, **40**, 327.
15 Y. R. Shen, *Nature*, 1989, **337**, 519.
16 R. A. Dluhy and D. G. Cornell, *J. Phys. Chem.*, 1985, **89**, 3195.
17 R. A. Dluhy, B. Z. Chowdhry and D. G. Cameron, *Biochim. Biophys. Acta*, 1985, **821**, 437.
18 R. A. Dluhy, *J. Phys. Chem.*, 1986, **90**, 1373.
19 R. A. Dluhy, N. A. Wright and P. R. Griffiths, *Appl. Spectrosc.*, 1988, **42**, 138.
20 R. A. Dluhy, M. L. Mitchell, T. Pettenski and J. Beers, *Appl. Spectrosc.*, 1988, **42**, 1289.
21 R. A. Dluhy, K. E. Reilly, R. D. Hunt, M. L. Mitchell, A. J. Mautone and R. Mendelsohn, *Biophys. J.*, 1989, **56**, 1173.
22 R. A. Dluhy, S. M. Stephens, S. Widayati and A. D. Williams, *Spectrochim. Acta, Part A*, 1995, **51**, 1413.
23 N. J. Harrick, *Internal Reflection Spectroscopy*, Wiley Interscience Publishers, New York, 1967.
24 P. Dumas, M. K. Weldon, Y. J. Chabal and G. P. Williams, *Surf. Rev. Lett.*, 1999, **6**, 225.
25 M. I. Tejedor-Tejedor and M. A. Anderson, *Langmuir*, 1986, **2**, 203.
26 A. J. McQillan, *Adv. Mater.*, 2001, **13**, 1034.
27 A. B. Horn and J. Sully, *J. Chem. Soc., Faraday Trans.*, 1997, **93**, 2741.
28 A. B. Horn and K. J. Sully, *Phys. Chem. Chem. Phys.*, 1999, **1**, 3801.
29 G. C. Pimentel and A. L. McClellan, *The Hydrogen Bond*, W. H. Freeman, San Francisco, 1960.
30 J. E. Bertie and Z. Lan, *Appl. Spectrosc.*, 1996, **50**, 1047.
31 N. Saliba, H. Yang and B. J. Finlayson-Pitts, *J. Phys. Chem. A*, 2001, **105**, 10 339.
32 H. Yang and B. J. Finlayson-Pitts, *J. Phys. Chem. A*, 2001, **105**, 1890.
33 T. Wilke, X. Gao, C. G. Takoudis and M. J. Weaver, *J. Catal.*, 1991, **130**, 62.
34 D. Krcho, *Kramers–Kronig Relations in Fourier Transform Infrared Spectroscopy of Semiconductors, The 3rd Biennial Engineering Mathematics and Applications Conference*, Adelaide, Australia, 1998.
35 K. Ohta and H. Ishida, *Appl. Spectrosc.*, 1988, **42**, 952.
36 M. J. Frisch, G. W. Trucks, H. B. Schlegel, P. M. W. Gill, B. G. Johnson, M. A. Robb, J. R. Cheeseman, T. Keith, J. A. Montgomery, K. Raghavachari, M. A. Al-Laham, V. G. Zakrzewski, J. V. Ortiz, J. B. Foresman, J. Cioslowski, B. B. Stefanov, A. Nanayakkara, M. Challacombe, C. Y. Peng, P. Y. Ayala, W. Chen, M. W. Wong, J. L. Andres, E. S. Replogle, R. Gomperts, R. L. Martin, D. J. Fox, J. S. Binkley, D. J. Defrees, J. Baker, J. P. Stewart, M. Head-Gordon, C. Gonzalez and J. A. Pople. *Gaussian 94*, rev. C.2, Gaussian, Inc., Pittsburgh, PA, 1995.
37 M. C. Goh, J. M. Hicks, K. Kemnitz, G. R. Pinto, K. Bhattacharyya and K. B. Eisenthal, *J. Phys. Chem.*, 1988, **92**, 5074.
38 M. C. Goh and K. B. Eisenthal, *Chem. Phys. Lett.*, 1989, **157**, 101.
39 Q. Du, R. Superfine, E. Freysz and Y. R. Shen, *Phys. Rev. Lett.*, 1993, **70**, 2313.
40 Q. Du, E. Freysz and Y. R. Shen, *Science*, 1994, **264**, 826.
41 J. P. Devlin and V. Buch, *J. Phys. Chem.*, 1995, **99**, 16 534.
42 J. P. Devlin, C. Joyce and V. Buch, *J. Phys. Chem. A*, 2000, **104**, 1974.
43 G. L. Richmond, *Annu. Rev. Phys. Chem.*, 2001, **52**, 357.
44 D. Maillard, M. Allavena and J. P. Perchard, *Spectrochim. Acta*, 1975, **31A**, 1523.
45 A. Schriver, L. Schriver and J. P. Perchard, *J. Mol. Spectrosc.*, 1988, **127**, 125.
46 G. Herzberg, *Molecular Spectra and Molecular Structure. II. Infrared and Raman Spectra of Polyatomic Molecules*, D. Van Nostrand Company, Inc., Princeton, NJ, vol. II, 1945.
47 M. Falk and P. A. Giguère, *Can. J. Chem.*, 1958, **36**, 1121.
48 A. R. Davis and R. M. Chatterjee, *J. Solution Chem.*, 1975, **4**, 399.
49 B. Meyer, M. Ospina and L. B. Peter, *Anal. Chim. Acta*, 1980, **117**, 301.
50 F. A. Cotton and G. Wilkinson, *Advanced Inorganic Chemistry*, John Wiley & Sons, New York, 2nd edn., 1966.
51 Q. Shi, P. Davidovits, J. T. Jayne, D. R. Worsnop and C. E. Kolb, *J. Phys. Chem. A*, 1999, **103**, 8812.
52 R. H. Maybury, S. Gordon and J. J. Katz, *J. Chem. Phys.*, 1955, **23**, 1277.
53 F. Fleyfel, H. H. Richardson and J. P. Devlin, *J. Phys. Chem.*, 1990, **94**, 7032.
54 M. Foster and G. E. Ewing, *Surf. Sci.*, 1999, **427–428**, 102.
55 M. C. Foster and G. E. Ewing, *J. Chem. Phys.*, 2000, **112**, 6817.
56 J. Boniface, Q. Shi, Y. Q. Li, J. L. Cheung, O. V. Rattigan, P. Davidovits, D. R. Worsnop, J. T. Jayne and C. E. Kolb, *J. Phys. Chem. A*, 2000, **104**, 7502.